Polymorphic phase behavior of lysophosphatidylethanolamine dispersions

A thermodynamic and spectroscopic characterization

James L. Slater,* Ching-hsien Huang,* Ralph G. Adams,‡ and Ira W. Levin‡

*Department of Biochemistry and Biophysics Program, University of Virginia School of Medicine, Charlottesville, Virginia 22908; and ‡Laboratory of Chemical Physics, National Institute of Diabetic, Digestive and Kidney Diseases, National Institutes of Health, Bethesda, Maryland 20892

ABSTRACT We have investigated the phase behavior of aqueous dispersions of a series of synthetic lysophosphatidylethanolamines as a function of the acyl chain length. Lysophosphatidylethanolamines exhibit phase polymorphism encompassing a well-ordered crystalline phase which may arise either from a metastable interdigitated lamellar gel phase or a metastable micellar phase. The time course of interconversion between these various phases have been outlined by observing the low temperature incubation time dependence of the calorimetric thermograms. We have determined differences in structure of these phases by Raman spectroscopy and ^{31}P nuclear magnetic resonance spectroscopy. It appears that a principal contribution to this polymorphic phase behavior lies in the nature of headgroup hydration and headgroup-headgroup interactions.

INTRODUCTION

Much of the accumulation of knowledge concerning the properties of lipid bilayers has focused on characterizing the behavior of the major lipid components existing within biological membranes. Exhaustive work utilizing various physical techniques has contributed greatly to the detailed understanding of the molecular behavior of these more abundant lipid species. Until recently, however, less attention has been directed towards understanding the behavior of the minor lipid components and how they function to influence membrane properties. A survey of the literature reveals that lysophospholipids, one class of these less abundant lipid species, have gained increasing popularity in recent biological and physical studies, perhaps owing to their possible role in membrane damage resulting during cardiac ischemia (Kako, 1986; Corr et al., 1982; Katz, 1982). The continual turnover of lipids via a reacylation-deacylation metabolic cycle provides a point of control for lysolipid concentration within membranes. This metabolic cycle may be temporally correlated with alterations in membrane permeability both in mitochondria (Wiswedel et al., 1982) and brain synaptosomes (Iwata et al., 1986), suggesting that membrane permeability may be controlled by utilizing lysolipids to affect membrane barrier properties.

Because lysolipids potentially exhibit detergentlike character, their concentrations must be carefully governed; when the membrane lysolipid concentrations exceed a threshold value, these single-chained amphiphiles disrupt membrane integrity. Erythrocyte membranes clearly undergo hemolysis at high lysolipid concentration (Weltzian et al., 1979) and exhibit profound changes in cell shape at much lower, sublytic concentrations (Ferrel et al., 1985; Fujii and Tamura, 1983). Perhaps other relevant biological functions of these lipids occur at concentrations below those which disrupt membrane integrity.

For example, lysolipids modulate the activity of membrane-bound enzymes (Weltzian et al., 1979; Weltzian and Munder, 1983). In particular, lysolipids affect the activity of the catalytic subunit of adenylate cyclase (Terman et al., 1985) and can competitively inhibit membrane bound acyltransferases (Weltzian and Munder, 1983). More recently, lysosphingolipids have emerged as potent inhibitors of protein kinase C (Hannun and Bell, 1987), implicating these lysolipids in the pathogenesis of various diseases resulting from sphingolipid accumulation. As a class of compounds, lysolipids and their various analogues display a diverse range of biological activities.

Investigations of macrophage chemotaxis reveal that macrophages may become activated to ingest target cells in response to exogenously added lysophospholipids (Ngwenya and Yamamoto, 1985; Yamamoto and Ngwenya, 1987). Similarly, lysolipid analogues containing an ether linkage in place of the usual sn-1 ester linkage demonstrate potent biological activity. Platelet activating factor (Benveniste and Vargaftig, 1983) is one well-known example. Additionally, covalently modified lysoplasmalogens exhibit antitumor properties (Weltzian and

Portions of this paper are derived from the dissertation of J. L. Slater presented in partial fulfillment of the requirement for a Ph.D. in biophysics, University of Virginia, January 1988.

Address reprint requests to Dr. Huang.

0006-3495/89/08/243/10 $2.00

Munder, 1983; Munder et al., 1987) resulting not only from disruption of the normal phospholipid metabolism, but also from their ability to transform macrophages into tumor-cytotoxic effector cells (Munder et al., 1987). All of these various biological phenomena suggest the likelihood of a class of receptors specific for lysolipids.

Understanding these diverse biological manifestations requires investigating the behavior of these lysolipids at the molecular level. These physical studies on aqueous lipid dispersions have already yielded a wealth of information concerning the behavior of phospholipids; furthermore, such understanding may yield additional insights concerning the development of novel liposomes. Our focus at present is to elucidate the phase behavior of lysophosphatidylethanolamines, thereby enabling a direct comparison of lysophosphatidylethanolamine properties with lysophosphatidylcholine properties determined by previous experimentation in our lab and other labs. Such comparisons concerning the phospholipid headgroup dependent phase behavior are already available for diacyl phospholipids. In our present study, particular attention is devoted towards dissecting the polymorphic phase behavior of the metastable intermediate states which appear in our system. The apparent phase behavior for these systems exhibiting metastable intermediates is determined in part by the previous treatment of the samples; in many cases, the system does not lie at a true thermodynamic equilibrium, but rather is still approaching equilibrium during the course of the experiment. Consequently, any characterization of the phase behavior concerning metastable intermediate states requires the knowledge of whether the experimental behavior reflects a true equilibrium system or whether the system is still evolving toward its final equilibrium position. We will demonstrate that these metastable intermediate states possess interesting properties and therefore deserve recognition in their own right.

MATERIALS AND METHODS

C(18)-, C(16)-, C(14)-, and C(12)-lysophosphatidylethanolamines (lyso-PE)[1] were purchased from Avanti Polar Lipids and used without further purification. All other chemicals used were either high purity (99.9+%) or else reagent grade.

Occasional spot checking of the sample purity by thin-layer chromatography (Kates, 1972) revealed no significant degradation products formed either during the sample preparation or during our experimental procedures. However, the potentially more serious problem of acyl chain or headgroup migration observed for lysophosphatidylcholines (Plückthun and Dennis, 1982) may result in significant sample heterogeneity. These various rearrangements produce positional isomers of the parent compound which are not easily resolved by thin-layer chromatography. However, the isotropic ^{31}P-NMR chemical shift differs slightly for the various isomers, and is therefore diagnostic for the presence of the rearrangement products. By this criterion, we have determined that under our experimental conditions, these rearrangement reactions do not occur appreciably with lysophosphatidylethanolamines.

Lipid dispersions were prepared with samples lyophilized from chloroform, then subsequently lyophilized from benzene before weighing. Two types of sample preparations, differing only in their thermal history, were utilized in these studies. The "nonhydrated" samples are dispersions prepared and maintained below the phase transition before experimental measurements. In contrast, "hydrated" samples are prepared by dispersing the lipid in solution, followed by several cycles of heating above the micellar phase transition temperature and cooling to O°C, thereby ensuring complete hydration of the samples before experimental measurements.

High sensitivity differential scanning calorimetry was performed using a model MC-2 equipped with the DA-2 digital interface and data acquisition utility (MicroCal, Inc., Amherst, MA). Scan rates in the range of 10°C/h to 30°C/h were utilized. Transition enthalpies and temperatures were determined using the software provided. The reported values of the T_m represent the temperature at maximum excess heat capacity. Because the reproducibility in high-sensitivity DSC may be limited by the accuracy of sample filling (Krishnan and Brandts, 1978), we performed multiple scans on a single sample to check these results against data obtained on independent samples. Calorimetry samples for determining the evolution of a metastable state as a function of an extended low temperature incubation period were preincubated within the calorimeter cell for time points <24 h; samples requiring more extensive low temperature incubation were held in an ice-water bath in the cold room before loading the preequilibrated calorimeter cell using an ice water jacketed syringe.

Phosphorus NMR was obtained using quadrature detection with a model FX-60Q multinuclear pulse Fourier transform spectrometer (JEOL USA, Cranford, NJ) operating at 24.15 MHz. All spectra were obtained using broadband noise decoupling of protons with a 5 KHz bandwidth at maximum decoupling power. A 90° pulse of 21 mS was used, with a 2.5-s delay between pulses. A typical spectrum accumulated 1,600 transients, each consisting of 8,000 data points collected at a digitizing rate of 50 mS per data point. Zero filling (Fukushima and Roeder, 1981) was utilized to enhance the signal-to-noise ratio, and no first order phase correction was introduced to the final spectrum. NMR samples were 100 mg/ml lyso-PE prepared with 1 mM EDTA as a chelator in 10% D_2O 90% H_2O.

Raman spectra were recorded at a resolution of 3–4 cm^{-1} as previously described using a Ramalog 6 spectrometer (Spex Industries, Inc., Edison, NJ) equipped with holographic gratings (Huang et al., 1982). The 514.5-nm line of either a model CR-12 (Coherent Inc., Palo Alto, CA) or an Innova 100 argon ion laser was used for excitation; ~200 mW of power was provided at the sample. The monochrometer was calibrated with atomic argon lines, and the frequencies are reported to ±2 cm^{-1}. Spectra were collected and stored on an LSI-11 based computer running an RT-11 operating system. Scan rates of 1 cm^{-1}/s were utilized for data collection; spectra reflect 4–10 signal averaged scans depending upon the sample. Data for constructing temperature

[1]Abbreviations used in this paper: C(x)-lyso-PE, lyso-PE with an acyl chain containing (x) carbons in the sn-1 position; CSA, chemical shift anisotropy ($\Delta\sigma$); ILG, interdigitated Lamellar Gel; lyso-PC, lysophosphatidylcholine; lyso-PE, lysophosphatidylethanolamine; PC, phosphatidylcholine; PE, phosphatidylethanolamine; ^{31}P-NMR, phosphorus-31 nuclear magnetic resonance spectroscopy; T_L, transition temperature for the lower endothermic phase transition in lyso-PE; T_H, transition temperature for the higher endothermic phase transition in lyso-PE; T_m, temperature at maximal excess heat capacity; $\Delta\sigma$, chemical shift anisotropy.

profiles were also recorded on a model 1877 Triplemate spectrograph (Spex Industries, Inc.) using a model 1420 intensified silicon photodiode detector (EG&G, Salem, MA). These data were acquired at a spectral resolution of 5–6 cm^{-1} by a local LSI-11 based computer communicating with a laboratory PDP 11-70 computer for data storage and manipulation. 15–30 mW of power at 514.5 nm were supplied to the sample by a model 165-07 laser (Spectra-Physics Inc., Mountain View, CA). Temperature-dependent scans were generated in an ascending mode with 4-min equilibration times between consecutive points at 1°C intervals. Sample temperatures were maintained within ±0.1°C.

Temperature profiles for the multilamellar assemblies were constructed from the 2,800–3,100 cm^{-1} C-H stretching mode spectra using Raman peak height intensity ratios I_{2935}/I_{2880} and I_{2850}/I_{2880} to represent acyl chain order/disorder parameters. The I_{2850}/I_{2880} intensity ratio reflects primarily lateral chain–chain interactions, whereas the I_{2935}/I_{2880} intensity ratio reflects interchain interactions with some superposition of intrachain *trans/gauche* rotational isomerization effects (Levin, 1984; Vincent and Levin, 1988).

RESULTS AND DISCUSSION

We have adopted the micellar phase of lyso-PE as a reference point to observe the calorimetric behavior of the system as the micellar phase is cooled to low temperature and preincubated before scanning. By varying this preincubation period at low temperature, we obtain a "snapshot" of the system as it evolves in time. These series of thermograms may then be used to reconstruct the relaxation behavior of the various metastable states.

Calorimetry data obtained using high resolution differential scanning calorimetry on a homologous series of lyso-PEs ranging in acyl chain length from C(12)- to C(18)- are summarized in Table 1. Calorimetric thermograms for C(16)-lyso-PE, a representative member of this homologous series is shown in Fig. 1. When hydrated micellar phase lyso-PE is cooled and scanned immediately upon temperature equilibration, a single endothermic transition is apparent (Fig. 1 *B*). If the same sample is preincubated at low temperature for increasing periods of time, the enthalpy change associated with this transition decreases concomitantly with the appearance of a second, higher temperature endothermic phase transition (Fig. 1, *C* and *D*). This calorimetric behavior immediately suggests that as the micellar reference phase is cooled, it spontaneously converts from the micellar phase to a metastable phase responsible for the low temperature endothermic transition. Maintaining this metastable state at low temperature allows its further conversion to a more stable phase responsible for the higher temperature endothermic phase transition. Furthermore, this high temperature endotherm resembles the single endotherm exhibited by nonhydrated samples (compare Fig. 1 *A* [nonhydrated] with *C–F*). However, hydrated samples preincubated at low temperature exhibit additional phase transitions not observed in the nonhydrated sample. These additional transitions always precede the main high temperature endotherm.

With the exception of C(12)-lyso-PE, all lyso-PE species we have studied exhibit similar thermotropic behavior; C(12)-lyso-PE exhibits only a single transition. The

TABLE 1 Molar enthalpies and transition temperatures

Acyl chain length	Transition enthalpy	Transition temperature
	kcal/mol	*°C*
C(12) nonhydrated	8.44	32.2
C(12) hydrated	10.13	32.6
C(14) nonhydrated	8.99	46.5
C(14) hydrated	3.6	18.0
	10.8 ± 0.8	46.4 ± 0.5
C(16) nonhydrated	9.2 ± 0.8	59.2 ± 0.2
C(16) hydrated	5.7 ± 0.4	39.7 ± 0.9
	9.1 ± 0.5	58.0 ± 0.4
C(18) nonhydrated	12.32	67.5
C(18) hydrated	5.6	55.7
	11.0	67.4

Summarized for calorimetry measurements made on a series of lyso-PEs varying in acyl chain length. Transition temperatures represent the temperature at the maximum of the excess heat capacity curve. Standard deviations are reported whenever multiple determinations (usually three to five samples) of a thermodynamic parameter were available. The second larger values in ΔH and T_m for hydrated samples were obtained by extrapolating the experimentally determined values at various times (see Fig. 1) to the limiting value of the maximum.

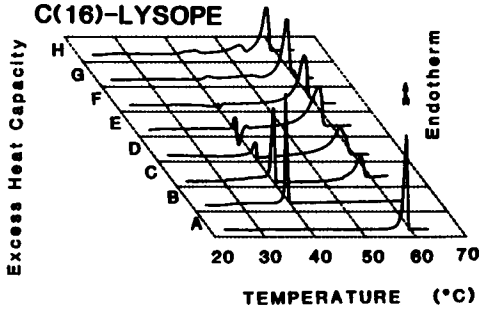

FIGURE 1 Thermograms are shown for samples of C(16)-lyso-PE as a function of the low-temperature preincubation period. Hydrated samples were cooled to the preincubation temperature from the micellar phase; the nonhydrated sample was prepared at and maintained at or below the preincubation temperature before scanning. The preincubation period is measured from the start of cooling to the start of the scan. Samples *A–F* were preincubated at low temperature within the calorimeter cell; samples *G* and *H* were preincubated in the cold room in an ice water bath. (*A*) Nonhydrated sample. (*B*) Hydrated sample, cooled to 1°C for 2 h. (*C*) Hydrated sample, cooled to 1°C for 4.7 h. (*D*) Hydrated sample, cooled to 1°C for 16.43 h. (*E*) Hydrated sample, cooled to 1°C for 18.67 h. (*F*) Hydrated sample, cooled to 1°C for 52 h. (*G*) Hydrated sample, cooled to 0.1°C for 17 d. (*H*) Hydrated sample, cooled to 0.1°C for >30 d.

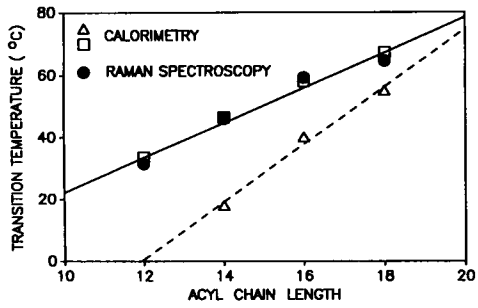

FIGURE 2 Phase transition temperatures are plotted as a function of the acyl chain length for both the low- and high-temperature endotherms. Values determined from calorimetry and from the temperature dependence of peak height intensity parameters calculated from Raman measurements on the C-H stretch region are shown.

temperature difference separating these two transitions decreases with increasing acyl chain length (Fig. 2), suggesting these two transitions merge in lyso-PE species with longer chain lengths; this phenomena has previously been recognized to occur in diacylPE (Chowdhry et al., 1984). Moreover, the indicated trend predicts the low temperature endotherm for C(12)-lyso-PE occurs below the lower limit (0°C) of temperature accessible with our calorimeter, explaining its apparent absence in our calorimetry studies. We may therefore divide the thermograms into three unique temperature regions: (*a*) $T < T_L$, temperatures below the lower endotherm (T_L); (*b*) $T_L < T < T_H$, temperatures between the two endotherms; (*c*) $T > T_H$, temperatures above the higher endotherm (T_H); where T_L is the low endothermic phase transition temperature and T_H is the high endothermic phase transition temperature. Our aim is to elucidate the structure of the phases present in each of these temperature domains by spectroscopic techniques, beginning with a determination of the temperature dependence of the ^{31}P-NMR lineshape, to distinguish the overall morphology of the phase present (Tilcock et al., 1986).

Fig. 3 displays the ^{31}P-NMR spectra obtained at different temperatures for a micellar sample cooled to 4°C. This spectral lineshape immediately observed upon cooling the micelles to 4°C indicates a bilayer morphology, and this lineshape persists up to 38°C. When the sample temperature is raised to 41°C, this broad lineshape indicative of a lamellar morphology narrows, confirming the presence of the phase transition already documented by calorimetry. The narrow isotropic lineshape of the reference micellar phase at 65°C indicates that lyso-PE indeed exists as micelles at temperatures above the high endothermic phase transition. We further investigated whether this phase behavior was reversible by obtaining the spectra with descending sample temperature. As lyso-PE is cooled from above the high endothermic transition temperature, the isotropic spectrum characteristic of micelles converts to the broad lineshape characteristic of the bilayer form when the sample temperature falls below the low endothermic phase transition temperature. The temperature dependence of the chemical shift anisotropy ($\Delta\sigma$) for C(16)-lyso-PE clearly indicates that this change in morphology of the phase occurs near the phase transition temperature.

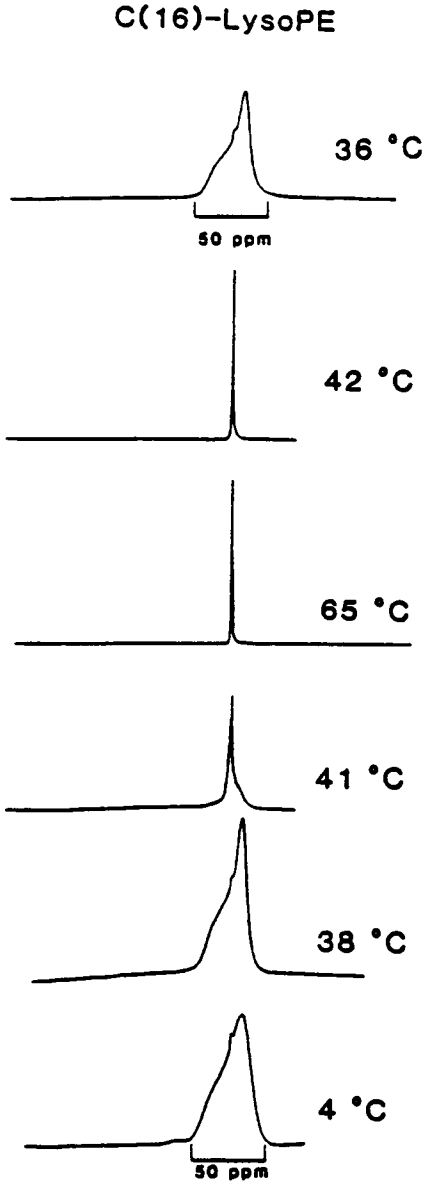

FIGURE 3 ^{31}P-NMR spectra for dispersions of C(16)-lyso-PE were taken sequentially at 4, 38, 41, 65, 42, and 36°C for a sample cooled from the micellar phase. The initial spectrum at 4°C was obtained as soon as the sample was cooled and temperature equilibrated. 1 h was allowed for stabilization of the instrument at subsequent temperatures before acquiring spectra.

The magnitude of the chemical shift anisotropy ($\Delta\sigma$) reflects the degree of motional averaging which is experienced by the phosphate moiety, and indicates the morphology of the phase within which the molecule resides (Tilcock et al., 1986). Raising the sample temperature to $T_L < T < T_H$ causes the collapse of the wide lineshape characteristic of the lamellar phase, giving rise to a sharp isotropic signal. This collapse of $\Delta\sigma$ indicates that the individual phospholipid molecules now exhibit a substantially greater degree of rotational and translational diffusion that is rapid enough that the molecules sample all orientations with respect to the magnetic field within the NMR timescale (Fyfe, 1983). This type of spectroscopic behavior is characteristic of a phase transition from a lamellar phase to a micellar or cubic phase (Eriksson et al., 1985). Our results, therefore, are consistent with a model that the lower temperature endotherm involves a transformation from a bilayer arrangement to a micellar phase displaying an isotropic ^{31}P-NMR spectrum.

In many respects, this lower endothermic phase transition observed in lyso-PE is analogous to the interdigitated lamellar gel to micellar phase transition observed for lysophosphatidylcholine (lyso-PC) (Wu et al., 1982). However, the similarity to lyso-PC ends here. If lyso-PE is maintained above the high endothermic transition temperature, the ^{31}P-NMR spectrum remains invariant, as it must for the micellar phase to serve as a stable reference point. In contrast, although lyso-PE maintained between the two endothermic transition temperatures never exhibit the lineshape characteristic of the lamellar phase, an additional broad component gradually appears in the spectrum with increasing incubation time, indicating a slow spontaneous conversion of the micellar phase to a stable phase whose spectroscopic character is distinguishable from either the micellar phase or the lamellar phase. Thus the micellar phase is metastable in the temperature region $T_L < T < T_H$ (Fig. 4 *A*). The large value of $\Delta\sigma$ (>200 ppm) associated with this broad spectral component is comparable to literature values reported for crystalline, anhydrous phospholipids (Griffin, 1976), suggesting that the metastable micellar phase relaxes to a solid phase exhibiting little or no axial motion. We will refer to this solid phase as the lyso-PE crystalline phase.

The slow rate of conversion of the micellar phase to this

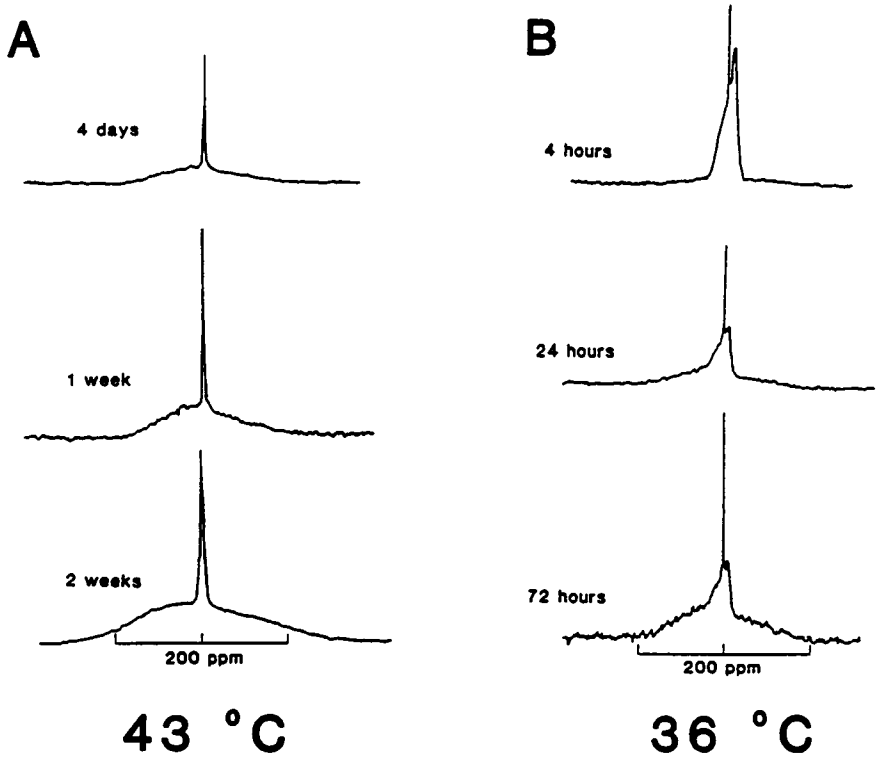

FIGURE 4 (*A*) Isothermal phase transition at 43°C is determined using ^{31}P-NMR for supercooled micellar C(16)-lyso-PE. An initially micellar sample was cooled to 43°C and the change in the ^{31}P-NMR spectrum was observed as a function of incubation time at this temperature. Data are presented for incubation periods of 4 d, 1 wk, and 2 wk at this temperature which corresponds to $T_L < T < T_H$. (*B*) Isothermal phase transition at 36°C is monitored using ^{31}P-NMR for supercooled micellar C(16)-lyso-PE. An initially micellar sample was cooled to 36°C and the change in the ^{31}P-NMR spectrum was observed as a function of incubation time at this temperature. Data is presented for a sample maintained for 4, 24, and 72 h at this temperature, which corresponds to $T < T_L$.

crystalline phase suggests that a large free energy barrier exists for the spontaneous conversion from the micellar phase to this crystalline phase. Furthermore, this crystalline phase is more stable relative to the metastable bilayer phase initially generated upon cooling the lyso-PE micellar phase below T_L, because the characteristic spectrum for this crystalline phase does not revert to the bilayer type spectrum even when the temperature is held below T_L. Our ^{31}P-NMR data suggest that this crystalline phase converts back to micelles above the high endothermic phase transition temperature (T_H), indicating that this high temperature endotherm detected calorimetrically must involve a transformation of crystalline lyso-PE to micellar lyso-PE. If indeed this crystalline phase is the most stable phase, a direct conversion of the lyso-PE lamellar phase to the crystalline phase must also be observable by ^{31}P-NMR. When lyso-PE is maintained in the temperature region $T < T_L$, the lamellar lineshape initially present also gradually acquires this additional broad ($\Delta\sigma > 200$ ppm) spectral feature, indicating that this crystalline phase may form directly from the bilayer phase (Fig. 4 *B*). Therefore, the bilayer phase initially generated when micelles are cooled below T_L is also metastable with respect to this crystalline phase. This result agrees with our calorimetry data. Although we believe both the metastable lamellar gel phase and the metastable micellar phase transform to the same crystalline phase, this conversion occurs more readily from the metastable bilayer phase.

By combining evidence from calorimetry and ^{31}P-NMR, it appears likely that the low temperature endothermic phase transition corresponds to a metastable bilayer to micellar phase transition, and the high temperature endothermic phase transition corresponds with a crystalline to micellar phase transition.

A comparison of $\Delta\sigma$ between lysolipids and diacyl lipids reveals that lysolipids experience an additional motion narrowing of the ^{31}P-NMR line shape in comparison to the diacyl lipids (Wu et al., 1984) (see Table 2). We believe that the unit undergoing axial rotation in the interdigitated lamellar gel phase of lysolipids may consist of a dimer of lipids, one from each monolayer; consequently, the observed motional narrowing is not simply the result of reducing the effective mass of the unit undergoing axial diffusion. Instead, this additional motion responsible for narrowing the spectrum in lysolipids may reside instead in a rotational motion about the C1-C2 bond of the glycerol backbone. This additional intramolecular rotational degree of freedom is expressed in lysolipids as a result of replacing the acyl chain in the sn-2 position by a single proton.

However, $\Delta\sigma$ for the broad spectral component representing the stable crystalline phase which gradually arises in lyso-PE is significantly greater than the value of $\Delta\sigma$ obtained for lyso-PC (Wu et al., 1982; Wu et al., 1984). Therefore, in the lyso-PE crystalline phase, this additional mechanism for motional averaging is inactive. Perhaps an additional hydrogen bonding interaction present in the lyso-PE headgroup, but absent in the lyso-PC headgroup prevents the onset of this additional rotational motion about the C1-C2 bond of the glycerol backbone in lyso-PE.

TABLE 2 Absolute values of the magnitude of ^{31}P-NMR chemical shift anisotropy

Lipid	Chemical Shift Anisotropy ($\Delta\sigma$)		Reference
	ppm	*phase*	
Diacyl-PE	45–60	Gel	1
	35–40	Fluid	
Lyso-PE	28–37	Metastable ILG	
	1–2	Isotropic	
	>200	Crystalline	
Diacyl-PC	230	Anhydrous	2
	55–69	Gel	1
	40–50	Fluid	1
Lyso-PC	30–40	ILG	3
	1	Micellar	

References: 1, Seelig, 1978; 2, Griffin, 1976; 3, Wu et al., 1984.

Molecular details concerning these interchain and intrachain order-disorder transitions (Levin, 1984; Wong, 1984) are revealed by examining the Raman spectra of lyso-PE. Extensive study of these vibrational transitions in lipid systems has determined that two peak height intensity ratios within the C-H stretching mode region (I_{2935}/I_{2880} and I_{2850}/I_{2880}) monitor both inter- and intrachain effects during the lamellar to micellar phase transition (Vincent and Levin, 1988).

Fig. 5 displays these temperature profiles constructed using these two peak height intensity ratios I_{2935}/I_{2880} and I_{2850}/I_{2880} obtained from spectra of C(16)-lyso-PE determined both after extensive preincubation at low temperatures (Fig. 5, *A* and *B*) and immediately after cooling the micellar solution (Fig. 5, *C* and *D*). Because this sample for Fig. 5, *C* and *D*, experienced no low temperature preincubation, the data represents primarily the lamellar gel to micellar phase transition. At this lamellar gel to micellar endothermic phase transition, each of these peak height intensity ratios increases, signifying that both the interchain and the intrachain disorder rise abruptly at the phase transition temperature. Above this phase transition temperature (41°C), these order parameters are comparable with values derived from similar measurements on other micellar phospholipid systems. Fig. 5, *A* and *B*, represent the temperature dependence of these peak height intensity ratios for a sample of lyso-PE cooled from the micellar phase and preincubated extensively at low

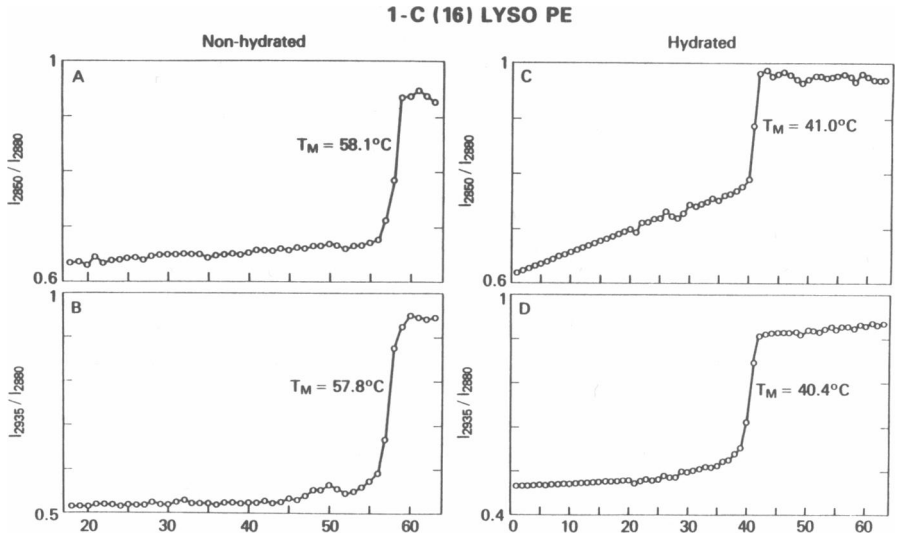

FIGURE 5 Temperature dependence of two peak height intensity ratio order parameters derived from the C-H stretching region are shown for C(16)-lyso-PE samples with either no low temperature preincubation or extensive low temperature preincubation. (*A*) I_{2850}/I_{2880} are plotted for a sample with extensive low temperature preincubation. The transition at 58.1°C confirms that the sample has largely converted to the crystalline phase. (*B*) I_{2935}/I_{2880} are plotted for a sample with extensive low temperature preincubation. The sample exhibits primarily the higher endothermic phase transition. (*C*) I_{2850}/I_{2880} are plotted for a sample with no low temperature preincubation. The sample exhibits only the low temperature endotherm, indicating that it is primarily in the metastable interdigitated lamellar gel phase. (*D*) I_{2935}/I_{2880} are plotted for a sample with no low temperature preincubation. This sample exhibits only the lower endothermic phase transition.

temperature. As expected, this predominantly crystalline phase sample undergoes an abrupt increase in these order parameters at 58.1°C, in good agreement with the high-temperature endothermic transition temperature observed calorimetrically. If the peak height intensity ratio is extrapolated to allow comparison at a common temperature with data from Fig. 5, *C* and *D*, we can support our model that the same micellar phase exists above either phase transition temperature. Comparing these intensity ratios below the transition temperature reveals that the lamellar gel phase (Fig. 5 *C*) exhibits more disorder than the crystalline phase (Fig. 5 *A*). However, these order parameters also indicate that the lyso-PE crystalline phase is considerably more disordered than other phospholipid crystalline phases.

The methylene deformation region of the Raman spectrum is potentially useful for distinguishing the type of acyl chain packing present in the hydrocarbon region of the bilayer. If micellar lyso-PE is cooled down and maintained below $T < T_L$, a spectrum of this deformation region indicates that initially the chain packing is hexagonally disordered (Fig. 6); upon extended low temperature incubation of this lamellar gel phase, a spectroscopic marker at 1,421 cm^{-1} gradually appears, signalling the presence of a very ordered orthorhombic or monoclinic hydrocarbon chain subcell. Therefore, the data from the deformation region of the spectrum demonstrates the

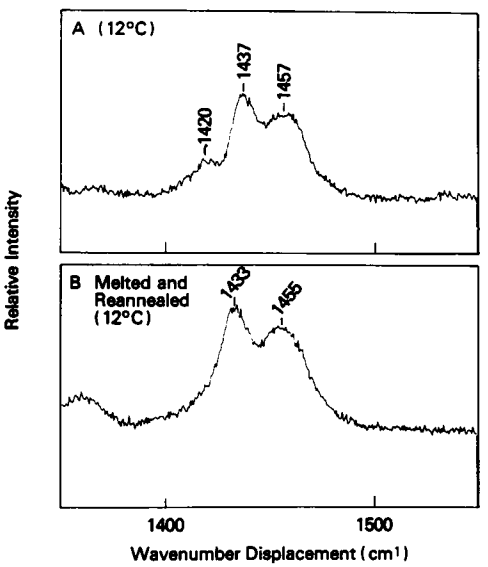

FIGURE 6 Raman spectra for the methylene deformation region for C(16)-lyso-PE is displayed as a function of low temperature preincubation. The appearance of the marker at 1,420 cm^{-1} signals the appearance of an orthorhombic or monoclinic subcell, indicating highly ordered packing of the hydrocarbon region of acyl chains. Spectrum A represents a sample which underwent extensive low temperature preincubation. Spectrum B was taken on the same sample immediately upon cooling from the micellar phase; the absence of the marker at 1,420 cm^{-1} indicates hexagonally packaged acyl chains.

gradual onset of orientationally ordered hydrocarbon packing upon extended low temperature preincubation. When this sample is then taken above the micellar phase transition and recooled, this indicator for orthorhombic packing is initially absent but gradually returns with low temperature preincubation.

Although the Raman order parameters obtained in the C-H stretching vibrations indicate that after prolonged low-temperature incubation, lyso-PE exhibits some conformational disorder of the acyl chains, the deformation region clearly indicates that the hydrocarbon packing is orientationally ordered. If we propose that acyl chain order depends on the depth within the bilayer hydrocarbon interior, different regions of the acyl chain may experience differing degrees of conformational order; although some residual conformational disorder is present in the crystalline phase, the acyl chains are packaged in the hydrocarbon lattice with orientational order.

It is generally recognized that lysophospholipids are capable of existing as micelles in aqueous solutions. For lyso-PC (Wu et al., 1982; Wu and Huang, 1983) and lyso-PE, both the values of the Raman order parameters above the high endothermic phase transition temperature, and the sharp isotropic ^{31}P-NMR resonances support the presence of micelles. Previous investigation on aqueous dispersions of lyso-PC have demonstrated that at low temperature, these micellar lipids spontaneously form a more stable phase consisting of a highly ordered interdigitated lamellar gel phase (Wu and Huang, 1983). Giving consideration to the headgroup dependent differences in phase behavior of the diacyl phospholipid species, and the previously published data on lyso-PC phase behavior, it is possible to construct a model for the lyso-PE phase behavior consistent with experimental results.

The lyso-PE micellar phase is only stable above the highest endothermic phase transition temperature ($T > T_H$). If these micelles are supercooled below this transition temperature ($T_L < T < T_H$), they become metastable with respect to the crystalline phase which arises directly from the micelles by slow interconversion. If these micelles are supercooled below the lower endothermic phase transition temperature ($T < T_L$), they become metastable with respect to a bilayer state, most probably with interdigitated acyl chains. If this metastable interdigitated lamellar gel phase (ILG phase) is heated, the micellar phase reappears as the sample undergoes the lower endothermic phase transition. However, extended low temperature preincubation of this metastable ILG phase results in its transformation of the crystalline phase. Upon heating, this crystalline phase contributes the high endothermic phase transition as it transforms back to the micellar phase. Therefore, the same crystalline phase may either arise directly from micelles, or via a metastable intermediate ILG phase. Our model is summarized in the entropy level diagram of Fig. 7.

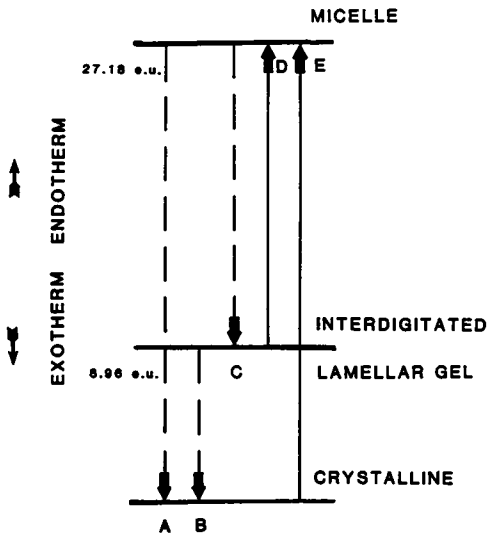

FIGURE 7 This entropy level diagram summarizes the relationship between various phases of C(16)-lyso-PE. The entropy values are derived from calorimetric data. Dotted lines (*A–C*) denote exothermic transitions, whereas solid lines (*D* and *E*) denote endothermic phase transitions. *D* corresponds to the low-temperature endothermic phase transition observed calorimetrically. *E* corresponds to the high-temperature endothermic phase transition observed calorimetrically. *A* represents the exothermic phase transition sometimes observed to overlap the low temperature endothermic phase transition. This exotherm represents the recruitment of newly formed micellar phase from transition *D* into the nucleated crystalline phase which already is present for samples with extensive low-temperature preincubation. Transition *C* may be observed with temperature scanning densimetry. Furthermore, there is evidence of transitions *A* and *B* from the isothermal ^{31}P-NMR experiments.

In addition to spectroscopy, other indirect evidence supports the existence of this crystalline phase in lyso-PE. For example, the rate of formation of the crystalline phase diacylPC decreases as the acyl chains are increased in length (Finegold and Singer, 1984). Increasing the acyl chain length in a homologous series of lyso-PE's results, as expected, in a correspondingly slower rate of conversion from the kinetically accessible metastable ILG state to the more thermodynamically stable, but kinetically limited crystalline phase.

DiacylPE also demonstrates polymorphic phase behavior, where the phase transition during the first heating scan for a nonhydrated sample occurs at a substantially higher temperature than the corresponding gel to liquid crystalline phase transition observed during subsequent calorimetric scans. This initially higher phase transition temperature may be interpreted as a simultaneous chain

melting and headgroup hydration transition (Mantsch et al., 1983; Xu et al., 1988), supported by the general notion that phase transitions occur at higher temperature as the headgroup region is generally dehydrated. DiacylPC systems under conditions of low water content exhibit substantially higher phase transition temperatures relative to the fully hydrated systems (Kodoma et al., 1982). These observations support our model that the lyso-PE crystalline phase is less hydrated relative to either the ILG phase or the micellar phase. Why is the lyso-PE crystalline phase stable at relatively high temperature?

Previously data from the diacylPE system reveals that in di-C(12)-PE, the gel phase which forms upon cooling the liquid crystalline phase is metastable, and may relax to form either of two distinct crystalline phases (Seddon et al., 1983). Upon heating, these crystalline phases convert directly to the liquid crystalline state without first passing thorugh the gel phase intermediate from which the crystalline phase was first derived. Moreover, this lower melting crystalline polymorph is metastable with respect to the higher melting crystalline polymorph, and appears to gradually convert to this higher melting polymorph given sufficient time. X-Ray data suggest also that the headgroup region of this higher melting crystalline polymorph is significantly less hydrated relative to all of the other phases. This pattern of metastability in these diacylPE systems is somewhat analogous to what we observe with our lyso-PE studies.

In contrast, crystalline phases for diacylPE with chain lengths of C(14) or greater appear not to undergo a phase transition directly to the liquid crystalline phase, but instead return to gel phase from which the crystalline phase was originally derived (Mulukutla and Shipley, 1984). Therefore, when the acyl chain length of diacylPE is shorter than C(12), the balance of forces results with headgroup–headgroup interactions predominating over the chain–chain interactions, enhancing the production of the variety of metastable intermediate states (Xu et al., 1988). Removing a single acyl chain to form the lyso-PE system would further enhance the importance of these headgroup–headgroup interactions relative to the chain–chain interactions, aligning the lyso-PE phase behavior more closely with the di-C(12)-PE rather than the longer chain length diacylPEs. However, removing an acyl chain to form lyso-PE also requires that the large cross-sectional area of the headgroup region relative to the acyl chain cross section contributed by a single chain must now be accommodated by either an unusually high degree of chain tilt relative to the bilayer normal, acyl chain interdigitation, or a combination of both (Hauser et al., 1981).

The bilayer spacing of C(18)-lyso-PC derived from low angle x-ray diffraction (Hui and Huang, 1986) indicate that the lyso-PC acyl chains are indeed interdigitated. Pending a similar study of lyso-PE, we may infer from these lyso-PC results that the acyl chains in our lyso-PE lamellar gel phase must also interdigitate.

Single crystal x-ray studies of the PC and PE headgroups have established a fundamental difference contrasting the headgroup–headgroup interactions present in these single component systems (Hauser et al., 1981). Although diacylPE may form hydrogen bonding and ionic interactions directly amongst neighboring headgroups, diacylPC headgroups contain no free hydrogen in the headgroup, and thus are incapable of participating directly as a hydrogen bond donor. Therefore, headgroup–headgroup interactions in diacylPC may only occur through the participation of intervening water molecules.

In conclusion, we propose that the metastable ILG phase in lyso-PE consists of highly hydrated headgroups, whose principal hydrogen bonding interactions are with water, rather than directly with neighboring headgroups. The process of forming the stable crystalline phase requires the headgroups to exchange these interactions with surrounding water molecules for the preferred participation in the direct headgroup–headgroup interaction expected in the crystalline phase. In contrast to the lyso-PC system which lacks this crystalline phase, lyso-PE is able to form the additional crystalline phase which is more stable relative to the ILG phase. This ability for lyso-PE to form this crystalline phase must result from the fundamental differences between the mode of headgroup–headgroup interaction for phosphatidylcholine headgroups and phosphatidylethanolamine headgroups.

This work was supported in part by United States Public Health Service grant GM-17452 from the National Institute of General Medical Sciences, National Institutes of Health, Department of Health and Human Services.

Received for publication 7 December 1988 and in final form 10 April 1989.

REFERENCES

Benveniste, J., and B. B. Vargaftig. 1983. Platelet-activating factor: an ether lipid with biological activity. *In* Ether Lipids: Biochemical and Biomedical Aspects. H. K. Mangold and F. Paltauf, editors. Academic Press, Inc., New York. 355–376.

Chowdhry, B. Z., G. Lipka, A. W. Dalziel, and J. M. Sturtevant. 1984. Multicomponent phase transitions of diacylphosphatidylethanolamine dispersions. *Biophys. J.* 45:901–904.

Corr, P. J., R. W. Gross, and B. E. Sobel. 1982. Arrythmogenic amphiphilic lipids and the myocardial cell membrane. *J. Mol. Cell. Cardiol.* 14:619–626.

Eriksson, P., G. Lindblöm, and G. Arvidson. 1985. NMR studies of 1-palmitoyllysophosphatidylcholine in a cubic liquid crystal with a novel structure. *J. Phys. Chem.* 89:1050–1053.

Ferrel, J. E., K. J. Lee, and W. A. Heustis. 1985. Membrane bilayer balance and erythrocyte shape: a quantitative assessment. *Biochemistry.* 24:2849–2857.

Finegold, L., and M. A. Singer. 1984. Phosphatidylcholine bilayers: subtransitions in pure and in mixed lipids. *Chem. Phys. Lipids.* 35:291–297.

Fujii, T., and A. Tamura. 1983. Dynamic behavior of amphiphilic lipids to penetrate into membrane of intact human erythrocytes and to induce change in cell shape. *Biomed. Biochim. Acta.* 42 (Suppl.):81–85.

Fukushima, E., and S. B. W. Roeder. 1981. Experimental Pulse NMR: A Nuts and Bolts Approach. Addison-Wesley Publishing Co., Reading, MA.

Fyfe, C. A. 1983. Solid State NMR for Chemists. CFC Press, Guelph, Ontario.

Griffin, R. G. 1976. Observation of the effect of water on the ^{31}P nuclear magnetic resonance spectra of dipalmitoyllecithin. *J. Am. Chem. Soc.* 98:851–853.

Hannun, Y. A., and R. M. Bell. 1987. Lysosphingolipids inhibit protein kinase C: implications for the sphingolipidoses. *Science (Wash. DC).* 23547:670–674.

Hauxser, H., I. Pascher, R. H. Pearson, and S. Sundell. 1981. Preferred conformation and molecular packing of phosphatidylethanolamine and phosphatidylcholine. *Biochim. Biophys. Acta.* 650:21–51.

Huang, C., J. R. Lapides, and I. W. Levin. 1982. Phase-transition behavior of saturated, symmetric chain phospholipid bilayer dispersions determined by Raman spectroscopy: correlations between spectral and thermodynamic parameters. *J. Am. Chem. Soc.* 104:5926–5930.

Hui, S. W., and C. Huang. 1986. X-Ray diffraction evidence for fully interdigitated bilayers of 1-stearoyllysophosphatidylcholine. *Biochemistry.* 25:1330–1335.

Iwata, H., A. Ohta, and A. Baba. 1986. Stimulatory effect of veratridine on lysophosphatidylethanolamine formation in rat brain synaptosomes. *Jpn. J. Pharmacol.* 41:293–297.

Kato, K. J. 1986. Membrane phospholipids and plasmalogens in the ischemic myocardium. *Can. J. Cardiol.* 23:184–194.

Kates, M. 1972. Techniques of lipidology: isolation, analysis and identification of lipids. Elsevier North-Holland Publishing Co., Amsterdam.

Katz, A. M. 1982. Membrane-derived lipids and the pathogenesis of ischemic myocardial damage. *J. Mol. Cell. Cardiol.* 14:627–632.

Kodama, M., M. Kuwabara, and S. Seki. 1982. Successive phase-transition phenomena and phase diagram of the phosphatidylcholine-water system as revealed by differential scanning calorimetry. *Biochim. Biophys. Acta.* 689:567–570.

Krishnan, K. S., and J. F. Brandts. 1978. Scanning calorimetry. *Methods Enzymol.* 49:3–14.

Levin, I. W. 1984. Vibrational spectroscopy of membrane assemblies. *Adv. Infrared Raman Spectrosc.* 11:1–48.

Mantsch, H. H., S. C. Hsi, K. W. Butler, and D. G. Cameron. 1983. Studies on the thermotropic behavior of aqueous phosphatidylethanolamines. *Biochim. Biophys. Acta.* 728:325–330.

Mulukutla, S., and G. G. Shipley. 1984. Structure and thermotropic properties of phosphatidylethanolamine and its *N*-methyl derivatives. *Biochemistry.* 2311:2514–2519.

Munder, P. G., M. Modelell, J. Storch, and W. Berdel. 1987. Alkyllysophospholipid in cancer therapy. *In* Present Status Non-Toxic Concepts Cancer. *International Symposium.* K.-F. Klippel and E. Macher, editors. S. Karger, New York.

Ngwenya, B. J., and N. Yamamoto. 1985. Activation of peritoneal macrophages by lysophosphatidylcholine. *Biochim. Biophys. Acta.* 839:9–15.

Plückthun, A., and E. A. Dennis. 1982. Acyl and phosphoryl migration in lysophospholipids: importance in phospholipid synthesis and phospholipase specificity. *Biochemistry.* 21:1743–1750.

Seddon, J. M., K. Harlos, and D. Marsh. 1983. Metastability and polymorphism in the gel and fluid bilayer phases of dilaurylphosphatidylethanolamine. *J. Biol. Chem.* 2586:3850–3854.

Seelig, J. 1978. ^{31}P nuclear magnetic resonance and the headgroup structure of phospholipids in membranes. *Biochim. Biophys. Acta.* 505:105–141.

Terman, B. I., A. J. Bitonti, J. Moss, and K. Vaughan. 1985. Activation and stabilization of the catalytic unit of adenylate cyclase. *Biochem. J.* 227:91–97.

Tilcock, C. P. S., P. R. Cullis, and S. M. Gruner. 1986. On the validity of ^{31}P-NMR determinations of phospholipid polymorphic phase behavior. *Chem. Phys. Lipids.* 40:47–56.

Vincent, J. S., and I. W. Levin. 1988. Interaction of ferricytochrome *c* with zwitterionic phospholipid bilayers: a Raman spectroscopic study. *Biochemistry.* 27:3438–3446.

Weltzian, H. U., and P. G. Munder. 1983. Synthetic alkyl analogs of lysophosphatidylcholine: membrane activity, metabolic stability and effects on immune response and tumor growth. *In* Ether Lipids: Biochemical and Biomedical Aspects. H. K. Mangold and F. Paultauf, editors. Academic Press, Inc., New York. 277–308.

Weltzian, H. U., G. Richter, and E. Ferber. 1979. Detergent properties of water-soluble choline phosphatides. *J. Biol. Chem.* 254:3652–3657.

Wiswedel, I., V. Barnstrorf, W. Augustin, E. Holmuhamedov, B. Medvedev, and Y. Eutodienko. 1982. Involvement of periodic deacylation-acylation cycle of mitochondrial phospholipids during Sr^{2+}-induced oscillatory ion transport in rat liver mitochondria. *Biochim. Biophys. Acta.* 688:597–604.

Wu, W., and C. Huang. 1983. Kinetic studies of the micellar to lamellar phase transition of 1-stearoyllysophosphatidylcholline dispersions. *Biochemistry.* 22:5068–5073.

Wu, W., C. Huang, T. G. Conley, R. B. Martin, and I. W. Levin. 1982. Lamellar-micellar transition of 1-stearoyllysophosphatidylcholine assemblies in excess water. *Biochemistry.* 21:5957–5961.

Wu, W., F. A. Stephenson, J. T. Mason, and C. Huang. 1984. A nuclear magnetic resonance spectroscopic investigation of the headgroup motions of lysophospholipids in bilayers. *Lipids.* 191:68–71.

Wong, P. T. T. 1984. Raman spectroscopy of thermotropic and high-pressure phases of aqueous phospholipid dispersions. *Annu. Rev. Biophys. Bioeng.* 13:1–24.

Xu, H., F. A. Stephenson, H. Lin, and C. Huang. 1988. Phase metastability and supercooled metastable state of diundecanoylphosphatidylethanolamine bilayers. *Biochim. Biophys. Acta.* 943:63–75.

Yamamoto, N., and B. Z. Ngwenya. 1987. Activation of mouse peritoneal macrophages by lysophospholipids and ether derivatives of neutral lipids and phospholipids. *Cancer Res.* 47:2008–2013.